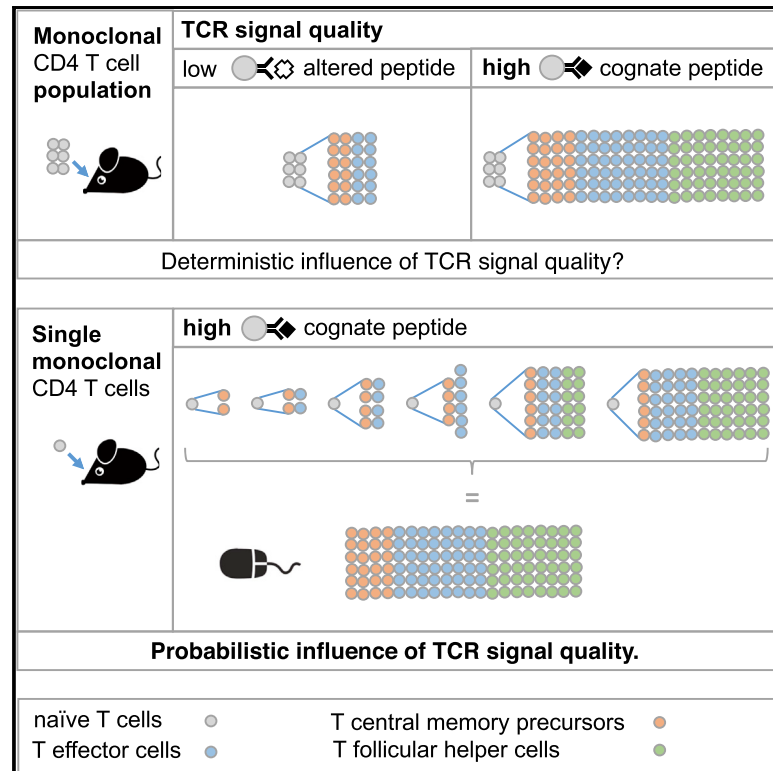


TCR Signal Quality Modulates Fate Decisions of Single CD4⁺ T Cells in a Probabilistic Manner

Graphical Abstract



Authors

Yi-Li Cho, Michael Flossdorf, Lorenz Kretschmer, Thomas Höfer, Dirk H. Busch, Veit R. Buchholz

Correspondence

dirk.busch@tum.de (D.H.B.),
veit.buchholz@tum.de (V.R.B.)

In Brief

The unique TCR expressed by a CD4⁺ T cell is thought to closely instruct its behavior in response to antigen encounter. Cho et al. question this deterministic concept by showing that single CD4⁺ T cells expressing identical TCRs take highly variable fate decisions when exposed to the same antigen *in vivo*.

Highlights

- Single CD4⁺ T cells take disparate fate decisions despite expressing identical TCRs
- A probabilistic model predicts the behavior of single TN and TCM cells
- Primary expansion into multiple memory cells enables reliable recall responses
- Polyclonal response patterns are predicted to segregate only upon recall



TCR Signal Quality Modulates Fate Decisions of Single CD4⁺ T Cells in a Probabilistic Manner

Yi-Li Cho,^{1,6} Michael Flossdorf,^{1,6} Lorenz Kretschmer,¹ Thomas Höfer,^{4,5} Dirk H. Busch,^{1,2,3,7,*} and Veit R. Buchholz^{1,7,8,*}

¹Institute for Medical Microbiology, Immunology and Hygiene, Technische Universität München (TUM), 81675 Munich, Germany

²Focus Group “Clinical Cell Processing and Purification,” Institute for Advanced Study, TUM, 85748 Munich, Germany

³National Center for Infection Research (DZIF), 81675 Munich, Germany

⁴Division of Theoretical Systems Biology, German Cancer Research Center (DKFZ), 69120 Heidelberg, Germany

⁵BioQuant Center, University of Heidelberg, 69120 Heidelberg, Germany

⁶These authors contributed equally

⁷Senior author

⁸Lead Contact

*Correspondence: dirk.busch@tum.de (D.H.B.), veit.buchholz@tum.de (V.R.B.)

<http://dx.doi.org/10.1016/j.celrep.2017.07.005>

SUMMARY

To what extent the lineage decisions of activated CD4⁺ T cells are determined by the quality of T cell receptor (TCR) ligation is incompletely understood. Here, we show that individual T cells expressing identical TCRs take highly variable fate decisions despite binding the same ligand. We identify a mathematical model that correctly captures this probabilistic behavior and allows one to formalize changes in TCR signal quality—due to cognate versus altered peptide ligation—as changes of lineage-specific proliferation and differentiation rates. We show that recall responses also adhere to this probabilistic framework requiring recruitment of multiple memory clones to provide reliable differentiation patterns. By extending our framework to simulate hypothetical TCRs of distinct binding strength, we reconstruct primary and secondary response patterns emerging from a polyclonal TCR repertoire *in silico*. Collectively, these data suggest that individual T cells harboring distinct TCRs generate overlapping primary differentiation patterns that segregate only upon repetitive immunization.

INTRODUCTION

In response to infection or vaccination, naive CD4⁺ T cells, which recognize their cognate antigen presented on major histocompatibility complex class II (MHCII) and receive further activating signals via co-stimulatory molecules and polarizing cytokines, proliferate and differentiate into defined T helper (Th) cell lineages. Binding of the T cell receptor (TCR) to its cognate peptide MHCII (p:MHCII) ligand sets off the proliferation of CD4⁺ T cells, while defined cytokines, secreted by antigen-presenting cells or bystander cells, induce T cell differentiation into Th1, Th2, Th17, T follicular helper (TFh), or induced T regulatory (iTreg) cells (Zhu et al., 2010). It has become increasingly clear that aside from polarizing cytokines, these lineage decisions are also influenced

by the strength of signals transmitted via the TCR (Kim and Williams, 2010; Tubo and Jenkins, 2014; van Panhuys, 2016). Strong TCR signals have been shown to favor differentiation into Th1 over Th2 cells (Evavold and Allen, 1991; Hosken et al., 1995; Jorritsma et al., 2003; van Panhuys et al., 2014), as well as Th17 over iTreg cells (Gomez-Rodriguez et al., 2009, 2014; lezzi et al., 2009), and are thought to be essential for differentiation into TFh cells (Baumjohann et al., 2013; Deenick et al., 2010; Fazilleau et al., 2009b; Hwang et al., 2015). TCR signal strength is determined by signal quantity and quality. Signal quantity is mainly influenced by the amount of cognate p:MHCII complexes available on an antigen-presenting cell (APC). In contrast, TCR signal quality is determined by the potency of the interaction between a given TCR and its p:MHCII ligand (Kim and Williams, 2010; Tubo and Jenkins, 2014; van Panhuys, 2016). On the molecular level, the potency of this interaction is best described by the aggregate dwell time of the TCR-p:MHCII complex (Govern et al., 2010). Vaccination studies have shown that TCR signal quality can substantially influence Th cell lineage decisions *in vivo* (Fazilleau et al., 2009b; Milner et al., 2010; Pfeiffer et al., 1995). It was found that populations of naive CD4⁺ T cells expressing a strongly binding transgenic TCR generate bigger burst sizes and stronger differentiation into TFh cells than T cell populations harboring a TCR that binds weakly to the same epitope (Fazilleau et al., 2009b). In addition, these data suggest that endogenous CD4⁺ T cells expressing TCRs of high binding strength are enriched in the TFh compartment (Fazilleau et al., 2009b).

Recently, p:MHCII multimer enrichment and subsequent limiting dilution-adoptive transfer of naive antigen-specific T cells have been combined to investigate the response patterns emerging from individual naive CD4⁺ T cells belonging to a polyclonal endogenous TCR repertoire (Tubo et al., 2013). It was found that average responses generated by populations of endogenous epitope-specific T cells showed robust differentiation patterns, while responses derived from single T cells expressing unique TCRs showed strong inter-clonal variation. These findings were taken as evidence that the behavior of an individual CD4⁺ T cell is closely determined by the nature of its TCR (Tubo et al., 2013). However, it was not assessed how much of the observed inter-clonal variation was indeed due to

TCR-dependent differences in signal quality, and how much of this variation on the single-cell level occurred independently of such differences.

To answer this open question, we first quantitated the differential effect of immunizing a monoclonal CD4⁺ T cell population with a cognate versus an altered peptide ligand. We then compared the magnitude of this effect to the magnitude of response variation emerging from single monoclonal T cells exposed only to the cognate peptide ligand. Starting out from naive T cell populations, we found that cognate versus altered peptide vaccination led to clear differences in peak expansion and to the emergence of characteristic differentiation patterns indicative of strong versus weak TCR ligation. However, individual naive CD4⁺ T cells showed massive inter-clonal variation when exposed to the same peptide ligand despite expressing identical TCRs. We identified a mathematical model that adequately described this probabilistic behavior of individual naive T cells and correctly predicted the strong response variation emerging from individual memory T cells, as well as the more reliable differentiation patterns generated by monoclonal memory populations. We further showed that changes in TCR signal quality—through cognate versus altered peptide ligation—can be formalized as changes of T cell subset-specific proliferation and differentiation rates. Based on these findings, we reconstructed *in silico* the response patterns emerging from a polyclonal TCR repertoire. This reconstruction predicted that the variable differentiation patterns derived from single naive T cells will strongly overlap during primary immune responses, but will segregate according to TCR signal quality when recall responses emerge from multiple memory cells.

RESULTS

Peptide Vaccination Induces T Central Memory Precursor, T Effector, and TFh Cells

We first performed a detailed phenotypic and functional characterization of a monoclonal population of T cells responding to vaccination with its cognate peptide. We sorted naive CD4⁺ T cells from OTII-TCR-transgenic-donor mice expressing the congenic marker CD45.1 and transferred these monoclonal T cell populations to C57BL/6 recipients. The OTII TCR binds to a peptide derived from chicken ovalbumin (OVA) that is presented on the I-Ab MHCII molecule of C57BL/6 mice (Robertson *et al.*, 2000). Recipients were immunized with this OVA_{323–339} wild-type peptide (OVA_{WT}) administered subcutaneously (s.c.) in complete Freund's adjuvant (CFA). At 8 days later, CD45.1⁺ T cell populations were monitored in lymph nodes draining the vaccination site. In order to characterize the phenotypic diversification of the response, we investigated the expression of surface markers CD62L and CXCR5. These have previously been suggested to divide CD4⁺ T cell populations at the peak of their response into CXCR5⁺CD62L[−] T effector (TEF) cells migrating into non-lymphoid organs, CXCR5⁺CD62L[−] TFh cells residing in or close to B cell follicles, and a subset of CD62L⁺ T cells capable of recirculating into lymph nodes from the blood stream (Fazilleau *et al.*, 2009a, 2009b). We found that our peptide vaccination scheme readily generated these three subsets (Figure 1A).

To probe the functional significance of the CD62L⁺ subset, we asked whether it contains precursors of long-lived T central memory (TCMp) cells, which have been shown previously to express lymph node homing markers such as CD62L and intermediate levels of CXCR5 (Pepper and Jenkins, 2011; Pepper *et al.*, 2011). At 8 days after primary vaccination, we sorted subsets according to their expression of CXCR5 and CD62L via flow cytometry (Figure 1B), transferred them into naive secondary recipients, and rested them for 35 days in the absence of antigen. Upon secondary immunization, we indeed found significantly stronger recall responses in recipients that had received CD62L⁺ T cells than in those that had received TFh or TEF cells (Figure 1C). Early CXCR5 expression did not appear to further segregate the recall capacity of the CD62L⁺ TCMP cells (Figures 1B and 1C). Closer investigation of the subset composition at the peak of the primary immune response revealed that the TEF subset contained both Th1 and Th17 cells expressing transcription factors T-bet and ROR γ t, respectively. TFh cells expressed high levels of their lineage-determining transcription factor Bcl-6, while TCMP and TEF cells expressed intermediate levels of this transcription factor (Figure 1D).

Thus, differential expression of CD62L and CXCR5 identifies TCMP, TEF, and TFh cells generated in response to vaccination with cognate peptide.

Average Response Patterns of T Cell Populations Are Closely Determined by TCR Signal Quality

We next compared the response patterns of monoclonal CD4⁺ T cell populations induced by a cognate peptide to those induced by TCR ligation with an altered peptide ligand (APL). We adoptively transferred 1,000 naive CD4⁺ T cells from OTII-donor mice expressing distinct combinations of congenic markers CD45.1/2 and CD90.1/2 (Figure S1). This allowed simultaneous tracking of eight T cell populations (A–H) within the same C57BL/6 recipient. Recipients were immunized with CFA plus either OVA_{WT} or the APL OVA_{R331}, in which histidine at position 331 is substituted by arginine (Robertson *et al.*, 2000). Importantly, binding of OVA_{WT} versus OVA_{R331} to the OTII TCR has recently been shown to induce strong versus weak TCR signaling characterized by the differential cleavage of Roquin and derepression of transcription factor IRF-4 (Jeltsch *et al.*, 2014). In line with such differential signal quality, the two immunizations induced progeny of distinct size and phenotype (Figures 2A and 2B): On average, population-derived responses against OVA_{WT} were 11 times larger than those induced by OVA_{R331} (Figure 2C). Further on, responses to OVA_{WT} were dominated by TEF and TFh cells, while TCMP cells constituted the smallest subset (“strong” response pattern: blue) (Figures 2A and 2D). In contrast, responses against OVA_{R331} were dominated by TCMP or TEF cells and contained very few TFh cells (“weak” response pattern: red) (Figure 2B and 2D). Progeny showing other subset compositions were rarely found (“other” response pattern: light blue) (Figure 2D). Importantly, when exposed to the same p:MHCII ligand, T cell populations generated similar burst sizes and subset compositions (Figures 2A–2D). Even reducing the administered dose of OVA_{WT} by 10-fold left the ensuing burst size and subset composition virtually unchanged (Figure S2).

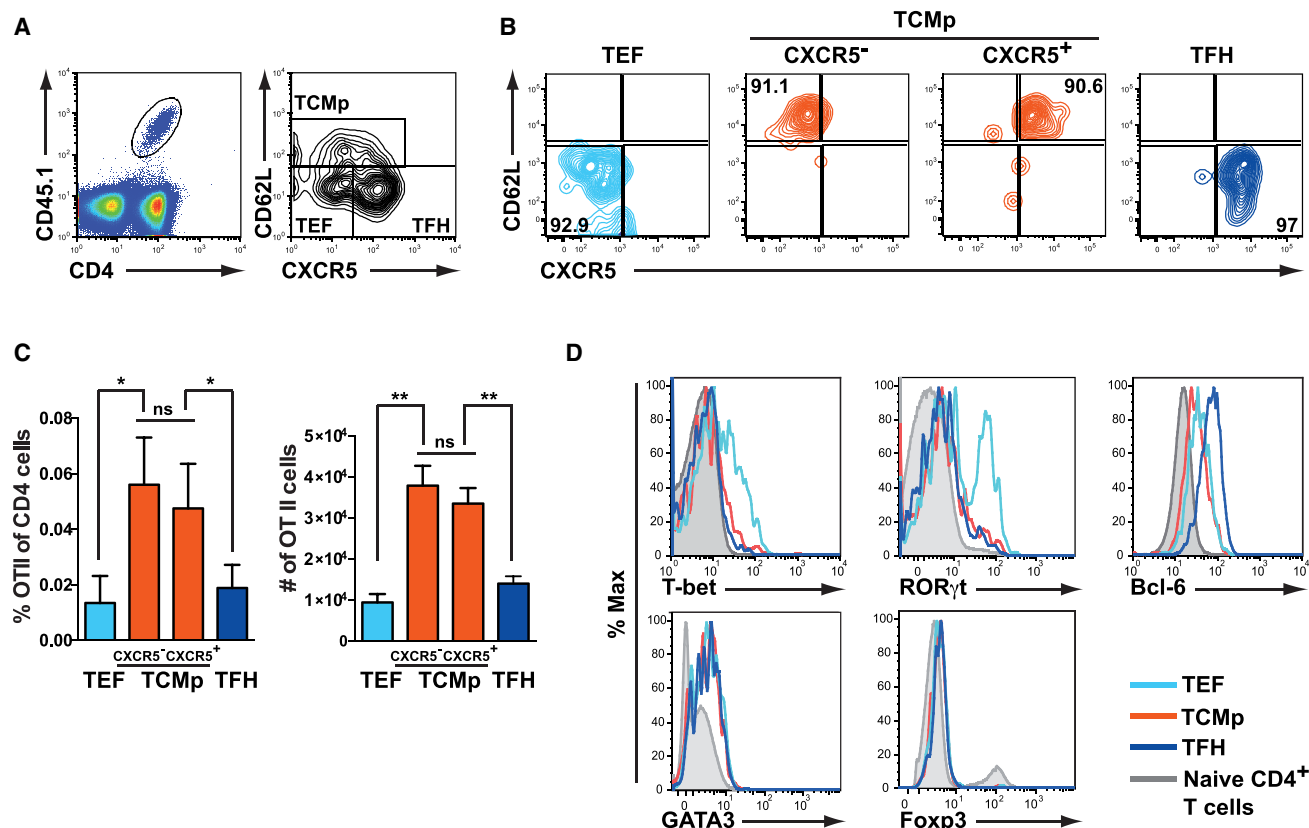


Figure 1. Peptide Vaccination Induces T Central Memory Precursor, T Effector, and Tfh Cells

(A–D) 10^4 naive $CD4^+CD25^-CD44^{lo}$ cells were sorted from peripheral blood of OTII-CD45.1-donor mice and adoptively transferred to C57BL/6 recipients, which were immunized s.c. at the tail base with OVA_{WT} in CFA. Immune responses were monitored in draining lymph nodes (dLNs) at day 8 post-immunization (p.i.). (A) Pseudo-color and contour plots show responding $CD4^+CD45.1^+$ T cells and their phenotypic subdivision into TEF ($CXCR5^-CD62L^-$), TCMp ($CD62L^+$), and TFh cells ($CXCR5^+CD62L^+$). (B and C) At day 8, p.i. antigen-experienced $CD4^+CD44^{hi}CD45.1^+$ T cells were sorted via flow cytometry into four subsets according to expression of CXCR5 and CD62L. 5,000 cells of these subsets were separately transferred into naive secondary C57BL/6 recipients and 35 days later exposed to intravenous (i.v.) recall immunization with modified vaccinia Ankara virus expressing OVA (MVA-OVA). (B) Contour plots indicate subset purity after flow cytometric sorting. (C) Bar graphs show mean recall expansion derived from transferred subsets at day 8 after recall immunization ($n = 3-4$). The error bars indicate SEM. (D) Histograms indicate expression of lineage defining transcription factors T-bet, ROR γ T, Bcl-6, GATA3, and Foxp3 at day 8 after primary immunization in OTII T cells of TEF, TCMp, and TFh phenotype and in naive endogenous $CD4^+$ T cells.

Together, these data confirm that the quality of the TCR:pMHCII interaction closely defines the outcome of immune responses derived from populations of monoclonal $CD4^+$ T cells.

Individual T Cells Take Highly Variable Fate Decisions Despite Receiving TCR Signals of Identical Quality

To investigate the impact of TCR signal quality on the fate decisions of individual $CD4^+$ T cells, we performed a series of single-cell-adoptive transfer experiments. In analogy to previous work on $CD8^+$ T cells (Buchholz et al., 2013; Graef et al., 2014), we isolated single naive $CD4^+$ T cells via fluorescence-activated cell sorting (FACS) from peripheral blood of eight OTII-congenic donors and simultaneously transferred these cells into C57BL/6 hosts. Size and phenotype of progeny derived from individual naive $CD4^+$ T cells were monitored in draining lymph nodes 8 days after vaccination with OVA_{WT} in CFA. We recovered pro-

geny of transferred individual T cells in 4.2% of cases. Accordingly, 8-fold single-cell transfers led to 68%, 30%, and 2% of recipient mice containing 0, 1, and 2 detectable progenies, respectively (Figure S3). Strikingly, we found that when exposed to the same p:MHCII ligand, single $CD4^+$ T cells harboring identical TCRs generated highly variable response sizes and differentiation patterns (Figures 3A–3D). This variation was not decreased when transferring single T cells from OTII-Rag1^{-/-} donors and thus was not dependent on expression of additional endogenous TCRs (Figures 3B–3D). At 180-fold, the inter-clonal variation between the largest and the smallest single T cell-derived progeny (Figure 3C) greatly exceeded the size difference attributed to the quality of TCR ligation on the population level (Figure 2C). Moreover, at least half of all single-cell-derived responses contained very few TFh cells and were categorized as weak despite resulting from TCR ligation with OVA_{WT} (Figure 3D).

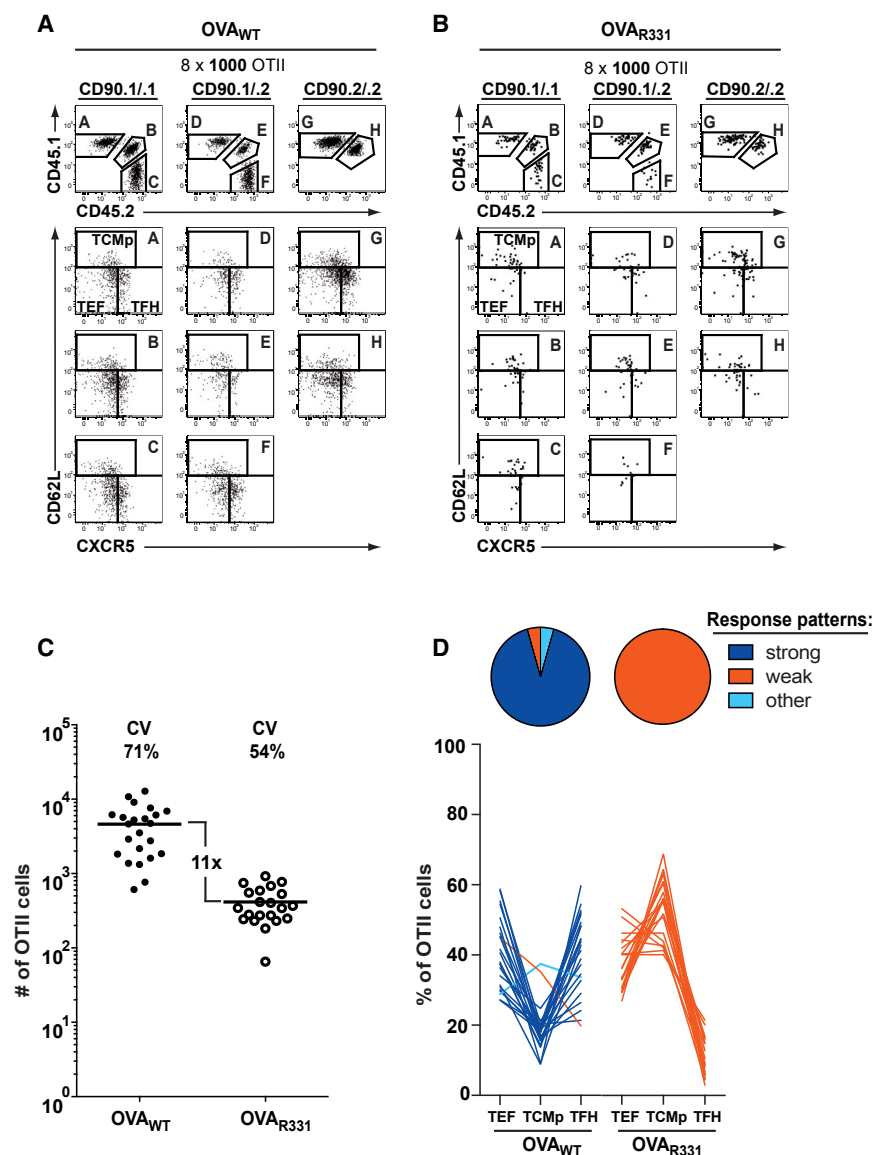


Figure 2. Average Response Patterns of T Cell Populations Are Closely Determined by TCR Signal Quality

(A–D) $8 \times 1,000$ $CD4^+CD25^-CD44^{lo}$ cells were sorted via flow cytometry from eight OTII-congenic donors expressing distinct combinations of congenic markers CD45.1/2 and CD90.1/2 and transferred to C57BL/6 recipients followed by s.c. immunization with 100 μ g of either OVA_{WT} or OVA_{R331} in CFA. Immune responses were analyzed in dLNs at day 8 p.i.

(A and B) Exemplary dot plots show congenic phenotype of recovered T cells (upper row) and expression of CXCR5 and CD62L in congenic populations A–H (lower three rows) after immunization with (A) OVA_{WT} in CFA or (B) OVA_{R331} in CFA.

(C) Scatterplots indicate absolute cell number recovered per transferred population. The bar indicates mean. CV: coefficient of variation.

(D) Line graphs indicate percentage of TEF, TCMp, and TFh cells within each responding population. Each line stands for one population. The response patterns are defined as strong (blue: TFh and TEF > TCMp), weak (red: TEF and TCMp \geq TFh), and other (light blue: remaining patterns). The pie charts show relative prevalence of response patterns.

See also Figures S1 and S2.

A Probabilistic Model Adequately Describes the Influence of TCR Signal Quality on Single T Cell Fate

In order to investigate whether the strong variation of progeny size and phenotype emerging from individual T cells is consistent with the closely defined response patterns generated by populations of $CD4^+$ T cells, we first reconstructed population responses in silico out of our single T cell-derived dataset. We assumed that the 4.2% of single-cell-adoptive transfers in which we detected progeny equate to the overall recovery rate upon

We also explored an alternative approach for fate mapping of single monoclonal T cells, similar to limiting dilution strategies previously applied by other research groups (Plumlee et al., 2013; Tubo et al., 2013). We chose conditions that guaranteed for more than 80% of recovered progenies to be genuinely derived from single naive T cells (Figure S4). This limiting dilution approach confirmed the inter-clonal variation in size (Figure 4A) and subset composition (Figure 4B) observed in our previous experiments and showed that such variation can also be detected when monitoring CXCR5 and PD-1 to dissect the formation of TFh and germinal center TFh cells (Figures 4C and 4D). However, without considering CD62L, this marker combination did not allow to clearly delineate TCMp from TEF and TFh cells and was thus, somewhat, less sensitive in detecting variation of single-cell-derived differentiation patterns.

adoptive transfer in our experimental system. This meant that transferring populations of 1,000 T cells led to responses composed out of an average of 42 single cells. Following these assumptions, we composed population responses in silico by repetitive random drawing from our single T cell-derived dataset and found composed responses to be in good accordance with the in vivo observations (Figure 5A). Thus, variable differentiation of single $CD4^+$ T cells expressing identical TCRs and exposed to the same cognate peptide did not occur randomly, but within a probabilistic framework that yielded predictable results when the response patterns of multiple T cells were cumulated.

A prototypical model of probabilistic cell differentiation assigns probabilities for differentiation and proliferation events of an individual cell within a given time interval, reflecting variable extrinsic stimuli and/or intrinsic cellular receptivity (Buchholz et al., 2013; Duffy et al., 2012; Feinerman et al., 2008). In

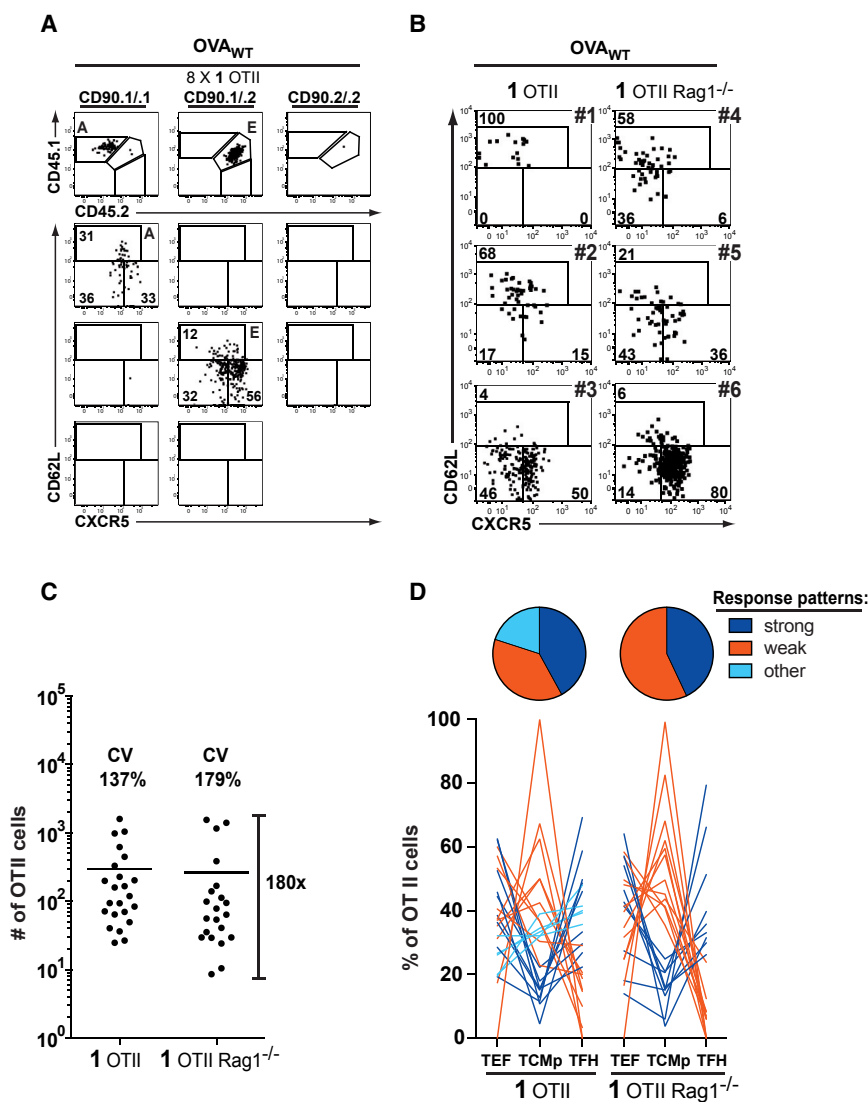


Figure 3. Individual T Cells Take Highly Variable Fate Decisions Despite Receiving TCR Signals of Identical Quality

(A–D) 8×1 $CD4^+CD25^-CD44^{lo}$ cells were sorted via flow cytometry from eight OTII or OTII-Rag1^{-/-}-congenic donors and transferred to C57BL/6 recipients followed by s.c. immunization with 10 μ g of OVA_{WT} in CFA. Immune responses were monitored in dLNs at day 8 p.i.

(A) Dot plots show congenic phenotype of recovered T cells (upper row) and expression of CXCR5 and CD62L in congenic populations (lower three rows). Note that two progenies recovered within the same recipient show distinct size and subset composition.

(B) Dot plots showing size and phenotype of progeny derived from single OTII (#1–3) or single OTII-Rag1^{-/-} cells (#4–6).

(C and D) As in Figures 2C and 2D, but instead showing progeny size and subset composition derived from single OTII or single OTII-Rag1^{-/-} cells after immunization with OVA_{WT} in CFA. Note 180-fold difference between largest and smallest single-cell-derived progeny. See also Figure S3.

addition, decisions to differentiate from one T cell subset into another may be constrained by the directionality of underlying developmental pathways (Buchholz et al., 2013; Flossdorf et al., 2015). We formulated two basic models that, in agreement with the data, generate both CD62L⁺ TCMp and CD62L⁻ non-TCMp cells from a single naive T cell, but differ in the sequence of subset emergence (Figure 5B). We determined the subset-specific proliferation and differentiation rates by fitting the two models to our single T cell-derived dataset (Figure S5A). While both models could describe key features of single T cell-derived progenies at day 8 post-immunization (p.i.) (Figure S5B), only the model in which CD62L⁺ TCMp cells give rise to CD62L⁻ non-TCMp cells (“model I”) correctly predicted the early dynamic changes of subset prevalence within a responding T cell population (Figure 5C). This suggests that the directionality of differentiation from TCM to T effector memory (TEM) cells, previously identified for mature memory subsets during recall responses (Pepper et al., 2011), is already engrained in the early develop-

mental relationship of TCMp and non-TCMp cells during the primary expansion phase. We tested the capacity of model I to simulate the distribution of expansion size and phenotypic composition measured for single-cell and population-derived responses (Figure 5D). Indeed, these simulations closely matched the distribution of single T cell-derived progenies observed in vivo (Figure 5E) and, by cumulating multiple simulations, captured the response patterns of T cell populations (Figures 5F and S6). We hypothesized that the changes in TCR signal quality that lead to distinct population-derived response sizes and phenotypes after immunization with OVA_{WT} versus OVA_{R331} (Figure 5G) can be formalized by fractional changes made to the subset-specific proliferation and differentiation rates previously identified. Implementing this assumption into the model (Table S1) enabled us to generate responses to OVA_{R331} in silico that agreed with the ones observed in vivo (Figure 5H). To test in how far the formal changes in subset-specific proliferation rates resembled the true proliferation activity of CD4⁺ T cells, we measured incorporation of bromodeoxyuridine (BrdU) in CD62L⁺ and CD62L⁻ subsets at day 6 after vaccination with OVA_{WT} or OVA_{R331}. Importantly, we found BrdU incorporation to be in good accordance with our predictions (Figure 5I). Thus, the same probabilistic framework was capable of describing the strong variation emerging from individual monoclonal T cells, as well as the robust response behavior of a T cell population and allowed us to quantify the effect of changing TCR signal quality on T cell proliferation and differentiation.

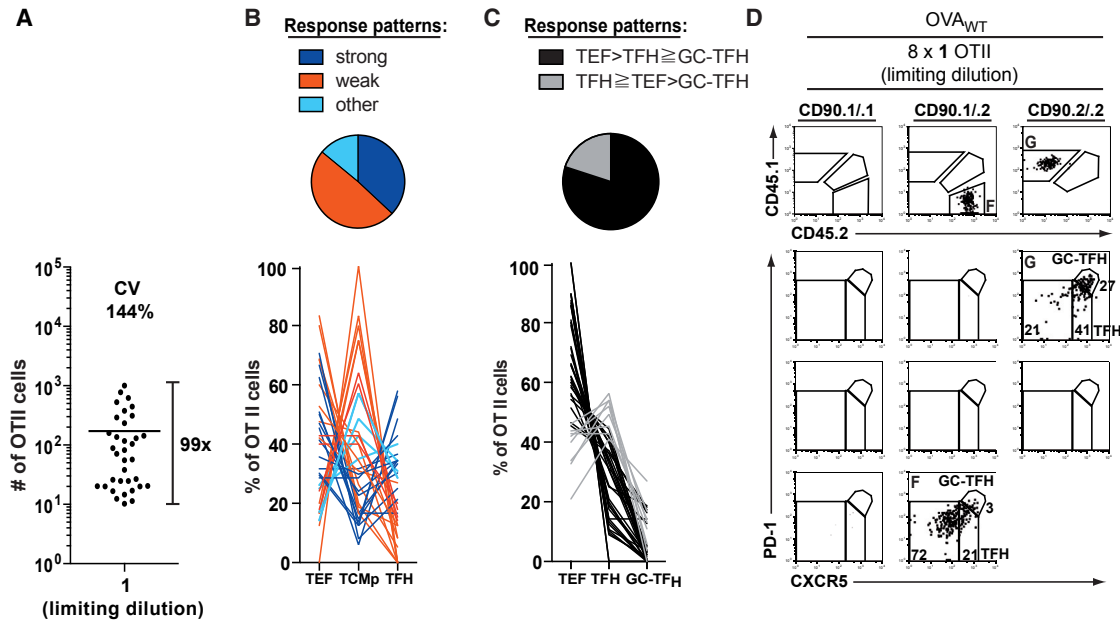


Figure 4. Limiting Dilution-Adoptive Transfer Confirms Variation in T Cell Response Size and Subset Composition

(A–D) 8×10 CD4⁺CD25⁻CD44^{lo} cells were sorted via flow cytometry from eight OTII-congenic donors expressing distinct combinations of congenic markers CD45.1/2 and CD90.1/2 and transferred to C57BL/6 recipients followed by s.c. immunization with 10 μ g of OVA_{WT} in CFA. Immune responses were monitored in dLNs at day 8 p.i.

(A and B) As in Figures 3C and 3D.

(C) Line graphs indicate percentage of TEF (CXCR5⁻PD-1⁻), TFH (CXCR5⁺PD-1⁻), and GC-Tfh cells (CXCR5⁺PD-1⁺) within each progeny. Each line stands for one progeny derived after limiting dilution-adoptive transfer. Response patterns are defined as indicated (black: TEF > TFH \geq GC-Tfh, gray: TFH \geq TEF > GC-Tfh). The pie charts show relative prevalence of response patterns.

(D) Congenic phenotype of recovered T cells (upper row) and expression of CXCR5 and PD-1 (lower three rows) delineating TFh and germinal center TFh (GC-TFH) cells. Of note, progenies derived after limiting dilution-adoptive transfer show distinct CXCR5/PD-1 phenotypes within the same recipient.

See also Figure S4.

Primary Expansion of a Unique CD4⁺ T Cell Clone into Multiple Memory T Cells Enables More Reliable Recall Responses

Based on the data gathered for primary immune responses, we hypothesized that the expansion of a unique CD4⁺ T cell clone into a population of memory T cells should allow for a more reliable influence of TCR signal quality on secondary immune responses. To test this hypothesis, we adoptively transferred limiting dilutions of naive OTII T cells and performed a primary immunization with modified vaccinia Ankara virus expressing OVA (MVA-OVA). 35 days later, we immunized the same recipients with OVA_{WT} plus CFA and compared ensuing responses in draining lymph nodes at day 8 after secondary vaccination to those generated by primary vaccination with the same peptide (Figure 6A). Interestingly, response sizes under both conditions varied across two orders of magnitude (Figure 6B) and thereby nearly matched variation of primary and secondary response sizes recently described for single polyclonal T cells and their progeny (Tubo et al., 2016).

In contrast, the differentiation patterns induced by secondary vaccination were substantially more robust than those found during primary immune responses. Primary vaccination with OVA_{WT} had yielded differentiation patterns, characterized by

weak TFh cell differentiation, in more than half of all detected progenies (Figure 6B). However, secondary immunization with the same peptide, preceded by primary vaccination with MVA-OVA, almost exclusively generated response patterns showing strong TEF and TFh cell differentiation and low percentages of TCMp cells (Figures 6B and 6C). We hypothesized that averaging the responses of multiple memory T cells would suffice to provide such robust secondary differentiation patterns. To also take into account the varying ratio of TCMp and non-TCMp cells, generated during primary responses, we simulated secondary responses emerging from populations of 100 memory T cells containing 0%–100% of TCM versus non-TCM cells. Assuming that TCM and non-TCM cells are characterized by the same proliferation and differentiation rates as their precursors, we applied the same model structure and parameters as learned for primary responses. Supporting these assumptions, we found that resulting simulations were in excellent accordance with the measured recall data (Figure 6D). To further exclude that the reliable regulation of secondary responses was mainly due to a per-cell differentiation bias imprinted during the primary response, we sorted TCM cells at day 35 after primary vaccination and adoptively transferred them into naive hosts via single-cell limiting dilution (Figure 6E). When exposing these single TCM cells to vaccination with OVA_{WT}, they generated highly variable

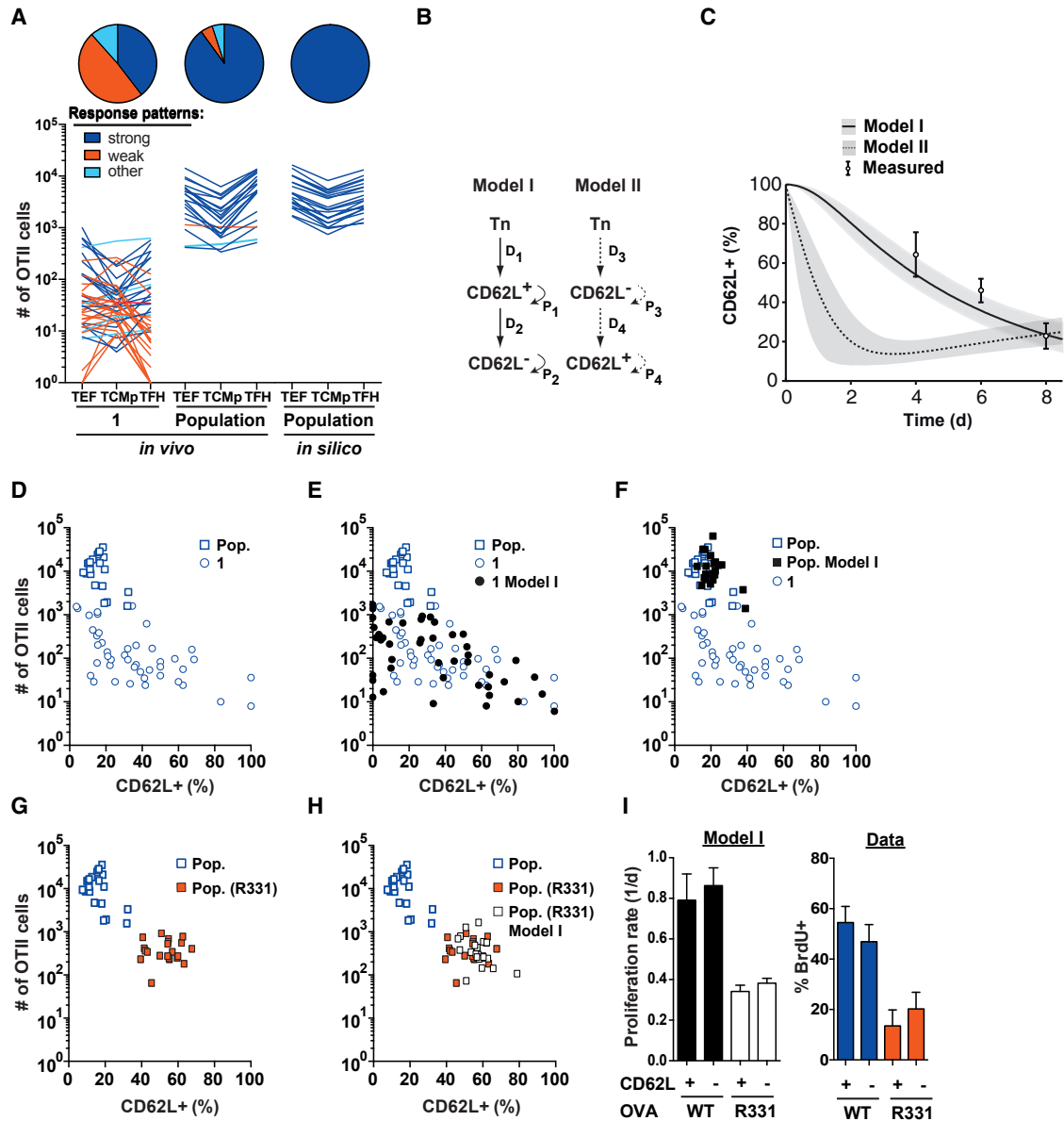


Figure 5. A Probabilistic Model Adequately Describes the Influence of TCR Signal Quality on Single T Cell Fate

(A) Line plots indicate absolute numbers of TEF, TCmp, and TFh cells recovered in dLNs after transfer of one (1) or 1,000 (population) OTII cells and immunization with 10 μ g of OVA_{WT} plus CFA or generated through in silico reconstruction of 1,000-cell transfers (population in silico) by cumulating on average 42 randomly drawn single-cell-derived responses do generate each line.

(B) Schematic depiction of two model structures in which CD62L⁻ arise from CD62L⁺ T cells (model I: full lines) or vice versa (model II: dashed lines). Differentiation and proliferation rates are indicated as D₁–D₄ and P₁–P₄.

(C) Percentage of CD62L expressing cells during the first 8 days p.i. as predicted by the two models and as measured after transfer of an OTII population (circles with error bars indicate mean and SD; filled regions indicate 95% confidence prediction bands).

(D–H) Scatterplots indicate the size (absolute cell number within dLNs) and phenotype (% CD62L positive cells) of progeny derived from single T cells (blue circles) or 1,000 adoptively transferred T cells after immunization with OVA_{WT} (blue squares) or OVA_{R331} (red squares).

(D) Data for single-cell- and population-derived responses to OVA_{WT}.

(E) Simulation of single-cell-derived responses using model I (black circles). Spearman correlation coefficient of data [95% confidence interval] and model: $r_{\text{Data}} = -0.52 [-0.71, -0.25]$, $r_{\text{Model}} = -0.31$.

(F) Simulation of population-derived responses by cumulating an average of 42 simulations from (E) (black squares): $r_{\text{Data}} = -0.27 [-0.64, 0.19]$, $r_{\text{Model}} = -0.13$.

(G) Data for population-derived responses to OVA_{WT} and OVA_{R331}.

(legend continued on next page)

differentiation patterns (Figures 6F and 6G) that were again in striking concordance with our model predictions (Figure 6H). Together, these data demonstrate that progenies of vastly different size and subset composition, derived from single monoclonal CD4⁺ T cells, will maintain their size differences, but display a shared differentiation pattern when secondary responses are averaged out of the probabilistic response patterns of multiple memory T cells.

Polyclonal Response Patterns Driven by Simulated TCRs of Distinct Binding Strength Segregate upon Secondary Expansion

To test the general relevance of our model framework, we next asked whether it could reproduce the primary and secondary differentiation patterns emerging from a polyclonal TCR repertoire. We reasoned that the model parameters identified for the interaction of the OTII TCR with distinct peptides (OVA_{WT} and OVA_{R331}) should also describe the TCR signal quality of two distinct TCRs interacting strongly or weakly with the same p:MHCII complex. To establish the model parameters for immunization with OVA_{R331}, the proliferation and differentiation rates defined for OVA_{WT} immunization had to be adapted by roughly the same factor -0.44 and 0.49 , respectively (Figure S1 and Table S1). To establish a set of hypothetical TCRs, we accordingly applied just one scaling factor per TCR. Using factors of 1, 0.81, 0.63, and 0.45, we generated TCRs of “high”, “intermediate-high”, “intermediate-low”, and “low” binding strength (Table S1). We then simulated the generation of CD62L⁺ TCMp and CD62L⁻ non-TCMp cells starting out from individual naive T cells harboring these distinct TCRs. Since TCM and TEM cells adoptively transferred during the memory phase have been reported to provide similar recall expansion (Pepper et al., 2011), we attributed the 5-fold lower recall capacity of non-TCMp versus TCMp cells that we had measured (Figure 1C) to their decreased survival in the absence of antigen. Accordingly, we reduced numbers of non-TCMp cells generated during primary simulations to a fifth and then simulated secondary responses starting out from the remaining TCMp and non-TCMp cells. As found in vivo (Tubo et al., 2016), these sequential simulations showed that primary differentiation patterns emerging from a polyclonal TCR repertoire partly determined ($r^2 = 0.61$) secondary differentiation patterns (Figure 7A). As expected, the predictive value of primary differentiation patterns further increased when the TCR signal quality of the responding progeny was known ($r^2_{hi} = 0.80$, $r^2_{int-hi} = 0.79$, $r^2_{int-lo} = 0.77$, $r^2_{lo} = 0.72$). However, these analyses only relate the behavior of primary and secondary progeny populations to each other. To more directly quantitate the differential impact of TCR signal quality on single-cell-derived responses, we asked how strongly the CD62L expression patterns of progeny derived from single T cells expressing distinct TCRs would overlap. In contrast to responses derived from ten naive T cells, we found that single T cells of

high versus low TCR binding strength generated strongly overlapping primary differentiation patterns (Simpson overlap coefficient [OC] = 60%). Importantly, these began to segregate during secondary immune responses, when more distinct differentiation patterns emerged as population averages, generated by multiple memory cells harboring the same TCR (OC = 27%) (Figure 7B).

DISCUSSION

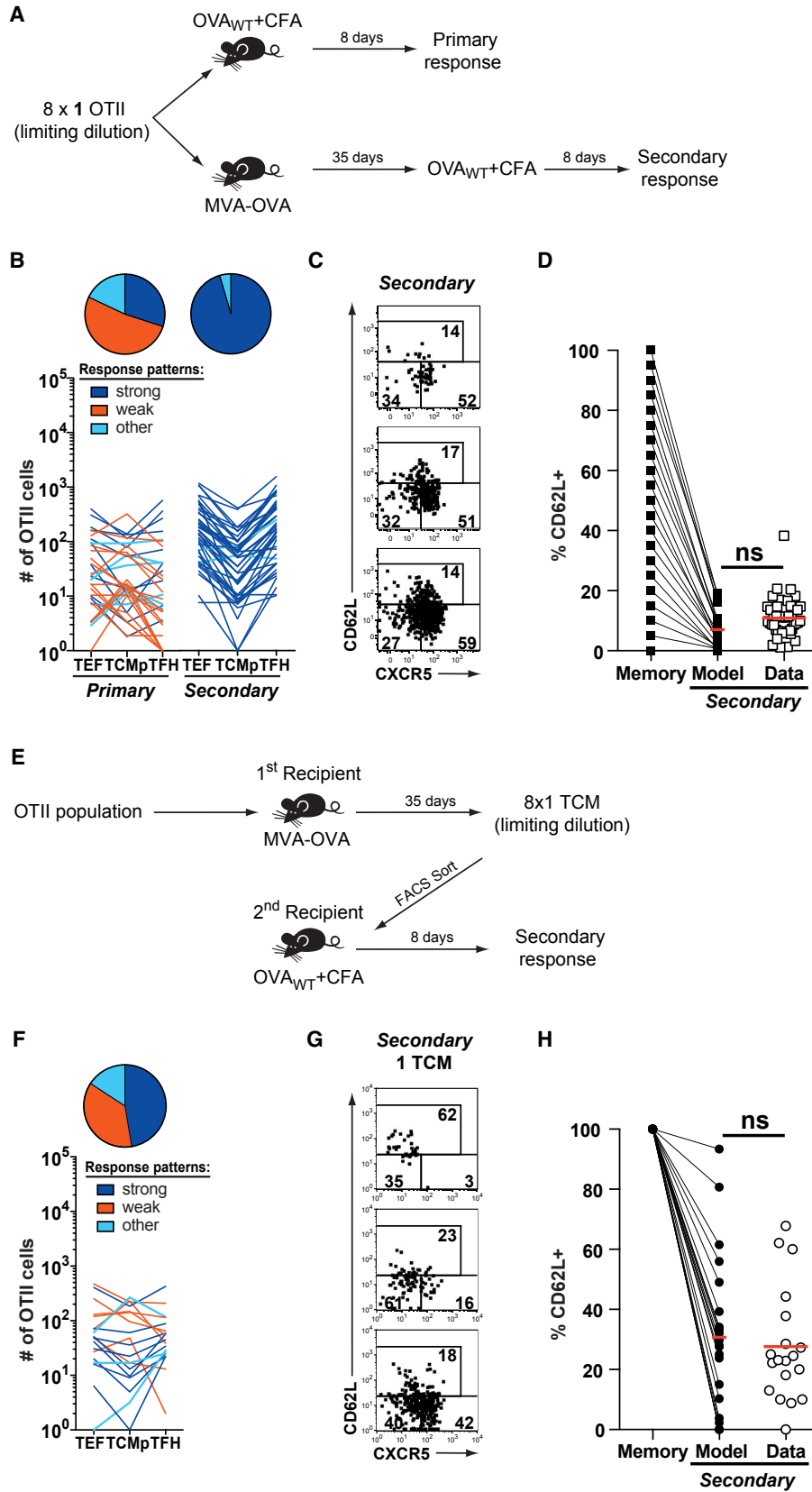
Of the 4×10^7 naive murine CD4⁺ T lymphocytes, no more than a few hundred cells harbor TCRs specific to a certain foreign peptide presented on MHCII (Jenkins et al., 2010; Moon et al., 2007). In addition, each one of the T cells belonging to such an epitope-specific population is thought to express a unique TCR that binds with distinct strength to its cognate p:MHCII ligand (Tubo and Jenkins, 2014; Tubo et al., 2013). Various studies conducted in vitro and in vivo have shown that the quality of TCR ligation influences the average expansion and differentiation of monoclonal CD4⁺ T cell populations (Boutin et al., 1997; Constant et al., 1995; Evavold and Allen, 1991; Fazilleau et al., 2009b; Jorritsma et al., 2003; Leitenberg et al., 1998). Recently, it has been shown that individual CD4⁺ T cells derived from a polyclonal endogenous repertoire generate progeny of vastly different size and phenotypic composition in response to TCR ligation with the same p:MHCII ligand (Tubo et al., 2013). However, it remained unclear how much of this interclonal variation was indeed driven by differences in TCR signal quality.

Studying immune responses derived from polyclonal single CD4⁺ T cells likely provides a mixed measure of effects attributable to the nature of the TCR and of effects driven by an unknown number of other deterministic or stochastic events that occur during the life history of an individual T cell. In our experimental system, we isolated the effect of TCR signal quality by measuring response patterns derived from a population of monoclonal naive CD4⁺ T cells exposed to either strongly or weakly binding peptide ligands. In such population-derived responses, individual fate-determining factors should be largely randomized and distinct response patterns can be attributed to differences in the binding strength of TCR ligation. Transgenic TCRs, such as 5CC7 and 2B4 binding to pigeon cytochrome C, as well as B3K506 binding to the peptides 3K, P5R, or P1-A, have been used previously to study the effects of differential TCR signal quality in vivo. In two recent studies, these systems have yielded differences in the mean expansion of T cell populations ranging between 2- to 4-fold and differences in the percentage of TFh or GC-TFh cells of approximately 3-fold (Fazilleau et al., 2009a; Tubo et al., 2013). Our experimental approach, based on studying OTII T cell responses against peptide vaccination with OVA_{WT} versus OVA_{R331}, generated differences in total population expansion of 11-fold and differences in the percentage

(H) Simulations of population-derived responses as in (E), but with reduced proliferation and differentiation rates (white squares): $r_{Data} = -0.02$ [$-0.44, 0.43$], $r_{Model} = -0.07$.

(I) Bar graphs show modeled mean proliferation rates and measured BrdU incorporation of CD62L⁺ and CD62L⁻ T cells 6 days after immunization with OVA_{WT} or OVA_{R331}. The error bars indicate 95% confidence bounds (for model I) and SEM (for data).

See also Figures S5 and S6; Table S1; and Supplemental Experimental Procedures.



(legend on next page)

of generated TFh cells of approximately 4-fold. Thereby, we covered a dynamic range of population expansion and differentiation similar to that interrogated by the aforementioned TCR-transgenic systems.

Strikingly, when mapping the fate of single CD4⁺ T cells expressing identical TCRs and exposed to the same p:MHCII ligand *in vivo*, we found that the size of their progeny varied by 180-fold, and the percentage of generated TFh cells varied by at least 21-fold. Thus, the quality of TCR ligation does not instruct the *in vivo* lineage decisions of an individual CD4⁺ T cell in a deterministic manner. These data rather argue that the influence, which a certain TCR has on the fate of an individual CD4⁺ T cell, is overlaid by probabilistic events occurring during the life history of this cell and that of its progeny.

These events may lie before, during, or after the onset of a single-cell-derived immune response (Beuneu et al., 2010; Lemaître et al., 2013). Mapping these events comprehensively; e.g., within the complex environment of a secondary lymphoid organ (Eickhoff et al., 2015; Qi et al., 2014) and combining this information with that on TCR signal quality, might in the future allow to retrospectively determine exactly why an individual CD4⁺ T cell has generated a certain response pattern. However, this insight will not allow answering prospectively which specific sequence of events a single naive T cell of defined TCR quality will encounter upon vaccination or infection. When taking into account these assumptions, our data argue that the outcome of immune responses derived from single CD4⁺ T cells must be considered as fundamentally uncertain.

In order to adequately describe both this fundamental uncertainty of single-cell-derived immune responses, as well as the impact of TCR signal quality on these responses, we developed a probabilistic computational model. This model allowed us to identify a basic developmental structure underlying the observed Th cell responses (i.e., differentiation of TCMp cells into non-TCMp cells) and further enabled us to extract and validate key parameters determined by strong versus weak TCR ligation (i.e., subset-specific proliferation and differentiation rates and their fractional alteration according to TCR signal quality). Importantly, the defined structure and parameters of this model learned on single-cell-derived primary immune responses sufficed to predict the course of secondary immune responses emerging from single TCMp cells, as well as the robust response patterns generated by monoclonal memory populations. These

findings are in line with data gathered for CD8⁺ T cells demonstrating that naive T cells differentiate first into memory precursor cells, some of which then give rise to shorter-lived effector cells (Badovinac et al., 2004, 2005; Buchholz et al., 2013; Joshi et al., 2007; Sarkar et al., 2008). In addition, immune responses derived from single monoclonal CD8⁺ T cells also show highly variable burst sizes and differentiation patterns (Buchholz et al., 2013; Gerlach et al., 2013; Graef et al., 2014) and have been best described by probabilistic models of proliferation and differentiation (Buchholz et al., 2013; Flossdorf et al., 2015; Marchingo et al., 2014).

A crucial question is how the variation in size and phenotype, observed for primary immune responses emerging from individual CD4⁺ T cells, translates to secondary immune responses derived from the daughter cells of these individual clones. Interestingly, we found that single-cell-derived progenies of vastly different size and subset composition will maintain their size differences (most likely due to maintenance of different numbers of memory precursors), but will display a shared differentiation pattern, during secondary immune responses. We utilized our theoretical framework to further extrapolate these insights to a polyclonal TCR repertoire. Importantly, our simulations of such a repertoire were guided by strict parameter extraction from our *in vivo* experiments. These simulations suggested that during primary responses, probabilistic effects independent of TCR quality strongly influence the course of single-cell-derived responses, thereby, creating a large overlap of differentiation patterns derived from clones of high versus low TCR binding strength. However, during recall immune responses, these effects move into the background and population-derived differentiation patterns segregate according to the quality of TCR ligation. Thus, the theoretical framework proposed here could explain why the dominance of high-avidity T cell clones within a polyclonal epitope-specific T cell response evolves only throughout repetitive immunizations (Busch et al., 1998; Savage et al., 1999). It would further suggest that the dominance of high-avidity clones evolves more quickly when multiple naive T cells expressing the same TCR exist in the naive repertoire. A recent study showed clear dominance of high-avidity CD4⁺ T cell clones without the need for repetitive immunization. Interestingly, this study employed an experimental system in which a fixed TCR alpha chain was used to reduce the diversity of the naive TCR repertoire (Kim et al., 2013). Such a redundant TCR

Figure 6. Primary Expansion of a Unique CD4⁺ T Cell Clone into Multiple Memory T Cells Enables More Reliable Recall Responses

(A) Schematic depiction of experimental setup: Sort and adoptive transfer were performed as in Figure 4, but half of recipients were primarily immunized with MVA-OVA (10⁸ pfu i.v.) rested for 35 days, recall immunized with OVA_{WT} in CFA, and analyzed 8 days later in dLNs.

(B) Line plots indicate absolute numbers of TEF, TCMp, and TFh cells recovered in dLNs after limiting dilution-adoptive transfer and primary or secondary immunization with OVA_{WT}.

(C) Exemplary dot plots show size and subset composition of progeny derived after secondary immunization.

(D) Starting out from hypothetical populations of 100 memory T cells containing 0%–100% of CD62L⁺ TCM cells (memory), secondary responses were simulated according to the structure and parameters of model I (see Figure 5B and Table S1), and the percentage of CD62L⁺ TCMp cells in simulated progeny (model) was compared to that generated during secondary responses *in vivo* (data).

(E) Schematic depiction of experimental setup: Populations of naive CD4⁺CD25[−]CD44^{lo} cells were sorted via flow cytometry from peripheral blood of OTII-congenic donors and transferred into primary recipients, which were then immunized with OVA_{WT} in CFA. At day 35 after immunization, congenic marker positive CD62L⁺ TCM cells were sorted from lymphatic tissues of primary recipients and adoptively transferred via single-cell limiting dilution into secondary recipients, which were subsequently immunized with OVA_{WT} in CFA. Secondary responses derived from single TCM cells were analyzed in dLNs at day 8 after vaccination. (F–H) As in (B)–(D), but secondary responses derived *in vivo* and simulated *in silico* starting out from single TCM cells. See also Table S1 and Supplemental Experimental Procedures.

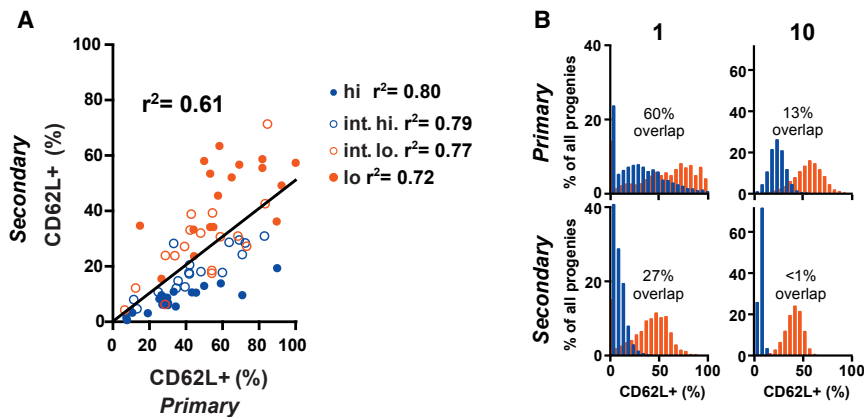


Figure 7. Polyclonal Response Patterns Driven by Simulated TCRs of Distinct Binding Strength Segregate upon Secondary Expansion

(A) Scatterplots depict percentage of CD62L⁺ T cells in simulated primary and secondary responses derived from individual naive T cells or their primary progeny, respectively. Responses of T cells harboring a hypothetical TCR of high binding strength are simulated according to the model structure and parameters of model I (see Figure 5B and Table S1). Primary and secondary responses of T cells harboring a hypothetical TCR of intermediate-high, intermediate-low, or low TCR binding strength are simulated according to the structure of model I, but with proliferation and differentiation rates (P1, P2, and D2) scaled by 0.81, 0.63, or 0.45, respectively.

(B) Bar graphs show percentage of CD62L⁺ T cells in simulated primary responses (upper row) derived from individual (1) or ten (10) naive T cells and simulated secondary responses (lower row) derived from the primary progeny of these T cells. At least 2,500 simulations were performed for each TCR. The resulting progenies were binned according to their percentage of CD62L⁺ T cells into bins spanning 5% intervals. The overlap between the resulting distribution of differentiation patterns induced by the two hypothetical TCRs (blue: high binding strength and red: low binding strength) was calculated according to the Szymkiewicz-Simpson coefficient.

repertoire should allow for a more rapid focusing on high-avidity clones by averaging the probabilistic response patterns of multiple naive T cells that express the same TCR.

From a clinical point of view, the data presented here shed light on the immunological principles underlying successful prime-boost vaccinations and have the potential to inform the design of future vaccination strategies that require optimally harnessing rare TCR specificities (Escolano et al., 2016).

EXPERIMENTAL PROCEDURES

Mice and Peptide Immunization

6- to 8-week-old C57BL/6 female mice were purchased from Envigo. OTII and OTII-Rag1^{-/-} mice expressing eight distinct congenic marker combinations of CD45.1, CD45.2, CD90.1, and CD90.2 were bred in-house at the animal facility of Technische Universität München. Animal care and experiments were in accordance with institutional protocols as approved by the relevant local authorities. For peptide immunization, C57BL/6 mice were injected s.c. at the tail base with 10–100 μg OVA_{WT} or OVA_{R331} plus CFA. For immunization with MVA-OVA, C57BL/6 mice were injected with 10⁸ pfu intravenously (i.v.).

Adoptive T Cell Transfer

Naive CD4⁺CD25⁻CD44^{lo} cells were purified from the peripheral blood of eight OTII or OTII-Rag1^{-/-} congenic-donor mice to >99% purity by flow cytometric cell sorting (MoFlo XDP, Beckman Coulter). Leukocytes from peripheral blood were stained with anti-CD44-fluorescein isothiocyanate (FITC) (IM4, eBioscience), anti-CD4-eF450 (RM4-5, eBioscience), and anti-CD25-APC (PC61, BD Biosciences) for 20 min at 4°C including propidium iodide (PI) labeling to discriminate dead cells. Naive CD4 cells (1, 10, or 1,000 cells) from eight OTII-congenic donors were consecutively sorted into the same well of a V-bottom 96-well plate, containing 200 μL of heat-inactivated fetal calf serum (FCS) and 4 × 10⁵ peripheral blood monocytes from C57BL/6 mice. Afterward, each well contained 8 × 1, 8 × 10, or 8 × 1,000 cells with distinct congenic phenotypes that were injected intraperitoneally (i.p.) into C57BL/6 mice.

Analysis via Flow Cytometry

At 8 days after OVA_{WT} or OVA_{R331} peptide immunization, lymphocytes were isolated from draining lymph nodes of C57BL/6 mice and homogenized by mechanical disruption on a sterile 70 μm cell strainer in RPMI 1640 medium

containing FCS. For antibody staining, 2 × 10⁷ cells were loaded into U-bottom 96-well plates and incubated with anti-CD16/32 (Fc-block; MR9-4, BD Biosciences) for 20 min. Subsequently, CXCR5 staining was performed in three successive steps by using anti-CXCR5-PE (SPRCL5, eBioscience) for 30 min, a secondary biotinylated-anti-PE (eBioPE-DLF, eBioscience) antibody for 20 min, and then with streptavidin-PE (BD Biosciences) in combination with any of the following labeling matrices: anti-CD45.1-FITC (A20, eBioscience), anti-CD90.1-FITC (OX7, BD Biosciences) or anti-CD62L-FITC (MEL-14, eBioscience), anti-CD19-PE CF594 (1D3, BD Biosciences), anti-CD45.1-PerCPy5.5 (A20, eBioscience), anti-CD62L-PE Cy7 (MEL-14, eBioscience) or anti-PD-1-PE Cy7 (J43, eBioscience), anti-CD45.2-Horizon V450 (104, BD Biosciences) or anti-CD45.1-eF450 (A20, eBioscience), anti-CD4-Pacific Orange (RM4-5, Invitrogen), anti-CD90.1-APC (HIS51, eBioscience), anti-CD27-APC (LG.7F9, eBioscience), or anti-CD62L-APC (MEL-14, eBioscience), and anti-CD90.2-APCeFluor780 (53-3.1, eBioscience) for 20 min. All staining procedures were performed at room temperature. For intracellular transcription factor staining, cells were first incubated with ethidium monazide (EMA) and Fc-block, then subjected to the 3-step CXCR5 staining procedure, as described, followed by staining of the surface markers anti-CD62L-FITC (MEL-14, eBioscience), anti-CD19-PE CF594, anti-CD4-Pacific Orange, and anti-CD45.1-APC (A20, eBioscience). In accordance with manufacturer guidelines, intracellular staining with anti-T-bet-BV421 (Apr46, BD Biosciences) or anti-Foxp3-eFluor 450 (FJK-16 s, eBioscience), anti-RORγt-APC (B2D, eBioscience), anti-GATA3-PECy7 (TWAJ, eBioscience), or anti-Bcl-6-PECy7 (K112-91, BD Biosciences) was performed at 4°C for 30 min after fixation and permeabilization.

Measurements were done on a 9-color CyAn ADP Flow Cytometer (Beckman Coulter). Analysis of FACS data was performed using Summit (Beckman Coulter) or FlowJo (Tree Star).

BrdU Incorporation

Mice were administered 1 mg bromodexoyridine (BrdU) i.p. and given 0.8 mg/mL BrdU plus 1 mg/mL sucrose in drinking water for 1 day before analysis. For BrdU analysis, the staining procedures were performed according to the BrdU Flow Kit (BD Biosciences) and included surface marker labeling as indicated above.

General Statistical Analysis

Unless otherwise indicated, statistical significance was determined by one-way ANOVA with Tukey's multiple comparison testing. Asterisks indicate statistical significance: * p < 0.05, ** p < 0.01, and *** p < 0.001.

SUPPLEMENTAL INFORMATION

Supplemental Information includes Supplemental Experimental Procedures, six figures, and one table and can be found with this article online at <http://dx.doi.org/10.1016/j.celrep.2017.07.005>.

AUTHOR CONTRIBUTIONS

Y.-L.C. designed and performed experiments and analyzed data; M.F. developed and performed the mathematical modeling approaches and analyzed data; L.K. performed experiments; T.H. developed the mathematical modeling approaches; and D.H.B. and V.R.B. developed the single-cell matrix approach, designed experiments, analyzed data, supervised the study, and wrote the paper.

ACKNOWLEDGMENTS

The authors thank L. Henkel and M. Schiemann for cell sorting; K. Molter for technical support; A. Muschawekch and I. Drexler for providing MVA-OVA; and K. Schober, S. Grassmann, K. Molter, and K. Wing for helpful discussion and/or critically reading the manuscript. The data presented in this manuscript are tabulated in the main paper and in the [Supplemental Information](#). This work was supported by the SFB 1054 (no. TP-B09), the SFB TR36 (no. TP-B10/13, TP-Z1), the Initiative and Networking Fund of the Helmholtz Association within the Helmholtz Alliance on Immunotherapy of Cancer, EU-FP7 SYBILLA (no. 201106), BMBF ForSysPartner (no. 0315267E), BMBF TIL-REP (no. 01ZX1403A), BMBF Quan-T-cell (no. 01ZX1505), and the National Science Foundation (no. NSF PHY11-25915).

Received: November 12, 2016

Revised: June 6, 2017

Accepted: June 30, 2017

Published: July 25, 2017

REFERENCES

- Badovinac, V.P., Porter, B.B., and Harty, J.T. (2004). CD8+ T cell contraction is controlled by early inflammation. *Nat. Immunol.* *5*, 809–817.
- Badovinac, V.P., Messingham, K.A.N., Jabbari, A., Haring, J.S., and Harty, J.T. (2005). Accelerated CD8+ T-cell memory and prime-boost response after dendritic-cell vaccination. *Nat. Med.* *11*, 748–756.
- Baumjohann, D., Preite, S., Reboldi, A., Ronchi, F., Ansel, K.M., Lanzavecchia, A., and Sallusto, F. (2013). Persistent antigen and germinal center B cells sustain T follicular helper cell responses and phenotype. *Immunity* *38*, 596–605.
- Beuneu, H., Lemaître, F., Deguine, J., Moreau, H.D., Bouvier, I., Garcia, Z., Albert, M.L., and Bousso, P. (2010). Visualizing the functional diversification of CD8+ T cell responses in lymph nodes. *Immunity* *33*, 412–423.
- Boutin, Y., Leitenberg, D., Tao, X., and Bottomly, K. (1997). Distinct biochemical signals characterize agonist- and altered peptide ligand-induced differentiation of naive CD4+ T cells into Th1 and Th2 subsets. *J. Immunol.* *159*, 5802–5809.
- Buchholz, V.R., Flossdorf, M., Hensel, I., Kretschmer, L., Weissbrich, B., Gräf, P., Verschoor, A., Schiemann, M., Höfer, T., and Busch, D.H. (2013). Disparate individual fates compose robust CD8+ T cell immunity. *Science* *340*, 630–635.
- Busch, D.H., Pilip, I., and Pamer, E.G. (1998). Evolution of a complex T cell receptor repertoire during primary and recall bacterial infection. *J. Exp. Med.* *188*, 61–70.
- Constant, S., Pfeiffer, C., Woodard, A., Pasqualini, T., and Bottomly, K. (1995). Extent of T cell receptor ligation can determine the functional differentiation of naive CD4+ T cells. *J. Exp. Med.* *182*, 1591–1596.
- Deenick, E.K., Chan, A., Ma, C.S., Gatto, D., Schwartzberg, P.L., Brink, R., and Tangye, S.G. (2010). Follicular helper T cell differentiation requires continuous antigen presentation that is independent of unique B cell signaling. *Immunity* *33*, 241–253.
- Duffy, K.R., Wellard, C.J., Markham, J.F., Zhou, J.H.S., Holmberg, R., Hawkins, E.D., Hasbold, J., Dowling, M.R., and Hodgkin, P.D. (2012). Activation-induced B cell fates are selected by intracellular stochastic competition. *Science* *335*, 338–341.
- Eickhoff, S., Brewitz, A., Gerner, M.Y., Klauschen, F., Komander, K., Hemmi, H., Garbi, N., Kaisho, T., Germain, R.N., and Kastenmüller, W. (2015). Robust anti-viral immunity requires multiple distinct T cell-dendritic cell interactions. *Cell* *162*, 1322–1337.
- Escolano, A., Steichen, J.M., Dosenovic, P., Kulp, D.W., Golijanin, J., Sok, D., Freund, N.T., Gitlin, A.D., Oliveira, T., Araki, T., et al. (2016). Sequential immunization elicits broadly neutralizing anti-HIV-1 antibodies in Ig knockin mice. *Cell* *166*, 1445–1458.e12.
- Evavold, B.D., and Allen, P.M. (1991). Separation of IL-4 production from Th cell proliferation by an altered T cell receptor ligand. *Science* *252*, 1308–1310.
- Fazilleau, N., Mark, L., McHeyzer-Williams, L.J., and McHeyzer-Williams, M.G. (2009a). Follicular helper T cells: lineage and location. *Immunity* *30*, 324–335.
- Fazilleau, N., McHeyzer-Williams, L.J., Rosen, H., and McHeyzer-Williams, M.G. (2009b). The function of follicular helper T cells is regulated by the strength of T cell antigen receptor binding. *Nat. Immunol.* *10*, 375–384.
- Feinerman, O., Veiga, J., Dorfman, J.R., Germain, R.N., and Altan-Bonnet, G. (2008). Variability and robustness in T cell activation from regulated heterogeneity in protein levels. *Science* *321*, 1081–1084.
- Flossdorf, M., Rössler, J., Buchholz, V.R., Busch, D.H., and Höfer, T. (2015). CD8+ T cell diversification by asymmetric cell division. *Nat. Immunol.* *16*, 891–893.
- Gerlach, C., Rohr, J.C., Perié, L., van Rooij, N., van Heijst, J.W.J., Velds, A., Urbanus, J., Naik, S.H., Jacobs, H., Beltman, J.B., et al. (2013). Heterogeneous differentiation patterns of individual CD8+ T cells. *Science* *340*, 635–639.
- Gomez-Rodriguez, J., Sahu, N., Handon, R., Davidson, T.S., Anderson, S.M., Kirby, M.R., August, A., and Schwartzberg, P.L. (2009). Differential expression of interleukin-17A and -17F is coupled to T cell receptor signaling via inducible T cell kinase. *Immunity* *31*, 587–597.
- Gomez-Rodriguez, J., Wohlfert, E.A., Handon, R., Meylan, F., Wu, J.Z., Anderson, S.M., Kirby, M.R., Belkaid, Y., and Schwartzberg, P.L. (2014). Itk-mediated integration of T cell receptor and cytokine signaling regulates the balance between Th17 and regulatory T cells. *J. Exp. Med.* *211*, 529–543.
- Govern, C.C., Paczosa, M.K., Chakraborty, A.K., and Huseby, E.S. (2010). Fast on-rates allow short dwell time ligands to activate T cells. *Proc. Natl. Acad. Sci. USA* *107*, 8724–8729.
- Graef, P., Buchholz, V.R., Stemmerger, C., Flossdorf, M., Henkel, L., Schiemann, M., Drexler, I., Höfer, T., Riddell, S.R., and Busch, D.H. (2014). Serial transfer of single-cell-derived immunocompetence reveals stemness of CD8+ central memory T cells. *Immunity* *41*, 116–126.
- Hosken, N.A., Shibuya, K., Heath, A.W., Murphy, K.M., and O'Garra, A. (1995). The effect of antigen dose on CD4+ T helper cell phenotype development in a T cell receptor-alpha beta-transgenic model. *J. Exp. Med.* *182*, 1579–1584.
- Hwang, S., Palin, A.C., Li, L., Song, K.-D., Lee, J., Herz, J., Tubo, N., Chu, H., Pepper, M., Lesourne, R., et al. (2015). TCR ITAM multiplicity is required for the generation of follicular helper T-cells. *Nat. Commun.* *6*, 6982.
- Iezzi, G., Sonderegger, I., Ampenberger, F., Schmitz, N., Marsland, B.J., and Kopf, M. (2009). CD40-CD40L cross-talk integrates strong antigenic signals and microbial stimuli to induce development of IL-17-producing CD4+ T cells. *Proc. Natl. Acad. Sci. USA* *106*, 876–881.
- Jeltsch, K.M., Hu, D., Brenner, S., Zöller, J., Heinz, G.A., Nagel, D., Vogel, K.U., Rehage, N., Warth, S.C., Edelmann, S.L., et al. (2014). Cleavage of roquin and regnase-1 by the paracaspase MALT1 releases their cooperatively repressed targets to promote T(H)17 differentiation. *Nat. Immunol.* *15*, 1079–1089.
- Jenkins, M.K., Chu, H.H., McLachlan, J.B., and Moon, J.J. (2010). On the composition of the preimmune repertoire of T cells specific for Peptide-major histocompatibility complex ligands. *Annu. Rev. Immunol.* *28*, 275–294.

- Jorritsma, P.J., Brogdon, J.L., and Bottomly, K. (2003). Role of TCR-induced extracellular signal-regulated kinase activation in the regulation of early IL-4 expression in naive CD4+ T cells. *J. Immunol.* *170*, 2427–2434.
- Joshi, N.S., Cui, W., Chandele, A., Lee, H.K., Urso, D.R., Hagman, J., Gapin, L., and Kaech, S.M. (2007). Inflammation directs memory precursor and short-lived effector CD8(+) T cell fates via the graded expression of T-bet transcription factor. *Immunity* *27*, 281–295.
- Kim, C., and Williams, M.A. (2010). Nature and nurture: T-cell receptor-dependent and T-cell receptor-independent differentiation cues in the selection of the memory T-cell pool. *Immunology* *131*, 310–317.
- Kim, C., Wilson, T., Fischer, K.F., and Williams, M.A. (2013). Sustained interactions between T cell receptors and antigens promote the differentiation of CD4+ memory T cells. *Immunity* *39*, 508–520.
- Leitenberg, D., Boutin, Y., Constant, S., and Bottomly, K. (1998). CD4 regulation of TCR signaling and T cell differentiation following stimulation with peptides of different affinities for the TCR. *J. Immunol.* *161*, 1194–1203.
- Lemaître, F., Moreau, H.D., Vedele, L., and Bousso, P. (2013). Phenotypic CD8+ T cell diversification occurs before, during, and after the first T cell division. *J. Immunol.* *191*, 1578–1585.
- Marchingo, J.M., Kan, A., Sutherland, R.M., Duffy, K.R., Wellard, C.J., Belz, G.T., Lew, A.M., Dowling, M.R., Heinzl, S., and Hodgkin, P.D. (2014). T cell signaling. Antigen affinity, costimulation, and cytokine inputs sum linearly to amplify T cell expansion. *Science* *346*, 1123–1127.
- Milner, J.D., Fazilleau, N., McHeyzer-Williams, M., and Paul, W. (2010). Cutting edge: lack of high affinity competition for peptide in polyclonal CD4+ responses unmasks IL-4 production. *J. Immunol.* *184*, 6569–6573.
- Moon, J.J., Chu, H.H., Pepper, M., McSorley, S.J., Jameson, S.C., Kiedl, R.M., and Jenkins, M.K. (2007). Naive CD4(+) T cell frequency varies for different epitopes and predicts repertoire diversity and response magnitude. *Immunity* *27*, 203–213.
- Pepper, M., and Jenkins, M.K. (2011). Origins of CD4(+) effector and central memory T cells. *Nat. Immunol.* *12*, 467–471.
- Pepper, M., Pagán, A.J., Igyártó, B.Z., Taylor, J.J., and Jenkins, M.K. (2011). Opposing signals from the Bcl6 transcription factor and the interleukin-2 receptor generate T helper 1 central and effector memory cells. *Immunity* *35*, 583–595.
- Pfeiffer, C., Stein, J., Southwood, S., Ketelaar, H., Sette, A., and Bottomly, K. (1995). Altered peptide ligands can control CD4 T lymphocyte differentiation in vivo. *J. Exp. Med.* *181*, 1569–1574.
- Plumlee, C.R., Sheridan, B.S., Cicek, B.B., and Lefrançois, L. (2013). Environmental cues dictate the fate of individual CD8+ T cells responding to infection. *Immunity* *39*, 347–356.
- Qi, H., Kastenmüller, W., and Germain, R.N. (2014). Spatiotemporal basis of innate and adaptive immunity in secondary lymphoid tissue. *Annu. Rev. Cell Dev. Biol.* *30*, 141–167.
- Robertson, J.M., Jensen, P.E., and Evavold, B.D. (2000). DO11.10 and OT-II T cells recognize a C-terminal ovalbumin 323-339 epitope. *J. Immunol.* *164*, 4706–4712.
- Sarkar, S., Kalia, V., Haining, W.N., Konieczny, B.T., Subramaniam, S., and Ahmed, R. (2008). Functional and genomic profiling of effector CD8 T cell subsets with distinct memory fates. *J. Exp. Med.* *205*, 625–640.
- Savage, P.A., Boniface, J.J., and Davis, M.M. (1999). A kinetic basis for T cell receptor repertoire selection during an immune response. *Immunity* *10*, 485–492.
- Tube, N.J., and Jenkins, M.K. (2014). TCR signal quantity and quality in CD4(+) T cell differentiation. *Trends Immunol.* *35*, 591–596.
- Tube, N.J., Pagán, A.J., Taylor, J.J., Nelson, R.W., Linehan, J.L., Ertelt, J.M., Huseby, E.S., Way, S.S., and Jenkins, M.K. (2013). Single naive CD4+ T cells from a diverse repertoire produce different effector cell types during infection. *Cell* *153*, 785–796.
- Tube, N.J., Fife, B.T., Pagán, A.J., Kotov, D.I., Goldberg, M.F., and Jenkins, M.K. (2016). Most microbe-specific naive CD4+ T cells produce memory cells during infection. *Science* *351*, 511–514.
- van Panhuys, N. (2016). TCR signal strength alters T-DC activation and interaction times and directs the outcome of differentiation. *Front. Immunol.* *7*, 6.
- van Panhuys, N., Klauschen, F., and Germain, R.N. (2014). T-cell-receptor-dependent signal intensity dominantly controls CD4(+) T cell polarization in vivo. *Immunity* *41*, 63–74.
- Zhu, J., Yamane, H., and Paul, W.E. (2010). Differentiation of effector CD4 T cell populations (*). *Annu. Rev. Immunol.* *28*, 445–489.